

Electronic Specific Heat of $\text{YBa}_2\text{Cu}_3\text{O}_{6+x}$ from 1.8 to 300 K

J. W. Loram, K. A. Mirza, J. R. Cooper, and W. Y. Liang

Interdisciplinary Research Center in Superconductivity, University of Cambridge, Madingley Road, Cambridge CB3 0HE, United Kingdom

(Received 27 August 1992; revised manuscript received 13 April 1993)

We have determined for the first time the “electronic” specific heat coefficient $\gamma(x, T)$ of $\text{YBa}_2\text{Cu}_3\text{O}_{6+x}$ for $0.16 \leq x \leq 0.97$ between 1.8 and 300 K. Weakly superconducting behavior between $x=0.43$ and 0.8 progresses rapidly to BCS-like superconducting and metallic normal state behavior for $x \geq 0.9$. However, the continuous development of the entropy $S(x, T)$ with x and T across the entire series suggests a progressive modification of the low energy spin spectrum with hole doping rather than a simple band model. Fermi statistics and k -space pairing are indicated by the magnitude and T dependence of $S(x, T)$.

PACS numbers: 65.40.Em, 74.20.Mn, 74.25.Bt

Fundamental questions relating to the normal and superconducting states of cuprate superconductors include the statistics of the carriers, the nature of the condensate (k -space pairing or condensation of real space bosons), the dominant low lying excitations, and the pairing mechanism. The specific heat (C) is a bulk thermodynamic quantity determined uniquely for any material by its spectrum of excitations, and the magnitude and temperature dependence of the electronic specific heat coefficient $\gamma = C^{\text{el}}/T$ provides an important test for proposed theories. Unfortunately the electronic term is only (1–2)% of the phonon term over most of the relevant temperature range and investigations of γ using conventional techniques are generally limited to the vicinity of the superconducting transition (for recent reviews see Refs. [1] and [2]). Using a high resolution differential technique [3] we determined [4] from 1.8 to 300 K the difference in electronic terms between $\text{YBa}_2(\text{Cu}_{1-y}\text{Zn}_y)_3\text{O}_{7-\delta}$ ($0 \leq y \leq 0.1$) and a $\text{YBa}_2(\text{Cu}_{0.93}\text{Zn}_{0.07})_3\text{O}_{7-\delta^*}$ reference sample for which superconductivity was almost entirely suppressed (δ and $\delta^* \sim 0.03$). The results were consistent with a T -independent normal state electronic term $\gamma_n \sim 1.6$ mJ/g-at. K^2 independent of Zn content for this fully oxygenated series. In this Letter we describe a detailed investigation using the same technique (and reference) of the specific heat of a ceramic $\text{YBa}_2\text{Cu}_3\text{O}_{6+x}$ sample for fifteen values of x in the range $0 \leq x \leq 0.97$. The differential method backs off most of the phonon specific heat [4], and with a correction for residual changes in phonon specific heat (found to scale with x), absolute values of the electronic term $\gamma(x, T)$ are determined spanning the entire system from antiferromagnetic (AF) insulator to slightly overdoped superconductor.

The ceramic $\text{YBa}_2\text{Cu}_3\text{O}_{6+x}$ (YBCO_{6+x}) sample of mass ~ 4 g was synthesized by conventional solid state reaction with x varied by annealing at appropriate temperatures in a suitable O_2 - N_2 atmosphere [5,6] and quenching into liquid N_2 . Values of x were determined with an uncertainty of around 0.01 relative to the initial fully oxygenated value ($x=0.97$) from changes in the sample mass. Measuring changes in specific heat with x

of a single sample minimizes uncertainties due to composition, anharmonicity, and nonintrinsic impurity and surface effects [1,2]. Measurements on ceramic samples are found to be as good (in zero magnetic field) as those on single crystals [1,2] and may benefit from more uniform oxygen stoichiometry. Resistivity, Hall effect, and thermopower data for a bar cut from the specific heat sample have been published [5] as has a discussion of the splitting of the superconducting transition [6] for $x > 0.92$ and an analysis of the fluctuation specific heat for $x \geq 0.87$ to obtain coherence lengths and Ginzburg temperatures [7]. (Values of oxygen deficiency δ in these previous publications are given by $\delta = 0.97 - x$.) We measure the ratio of the heat capacities of the $\text{YBa}_2\text{Cu}_3\text{O}_{6+x}$ sample and a fully oxygenated $\text{YBa}_2(\text{Cu}_{0.93}\text{Zn}_{0.07})_3\text{O}_{6.97}$ reference with resolution $1:10^4$ above 30 K, and also their total heat capacities. These results are combined (using the masses and atomic weights) to give the difference $\gamma^{\text{tot}}(x, T) - \gamma_{\text{ref}}^{\text{tot}}(T)$, where $\gamma^{\text{tot}} = C^{\text{total}}/T$.

Raw data for $\gamma^{\text{tot}}(x, T) - \gamma_{\text{ref}}^{\text{tot}}(T)$ are shown in Fig. 1

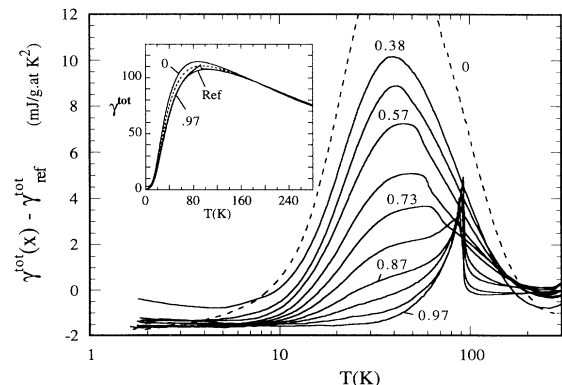


FIG. 1. $\gamma^{\text{tot}}(x) - \gamma_{\text{ref}}^{\text{tot}}$ vs T , where $\gamma^{\text{tot}} = C^{\text{total}}/T$, showing raw specific heat data for $\text{YBa}_2\text{Cu}_3\text{O}_{6+x}$ relative to the $\text{YBa}_2(\text{Cu}_{0.93}\text{Zn}_{0.07})_3\text{O}_{6.97}$ reference for $x = 0, 0.38, 0.48, 0.57, 0.67, 0.73, 0.80, 0.87, 0.92, 0.95, \text{ and } 0.97$. The closely spaced experimental points are joined for clarity. Inset: $\gamma^{\text{tot}}(x)$ for $x = 0, 0.50, \text{ and } 0.97$, and $\gamma_{\text{ref}}^{\text{tot}}$.

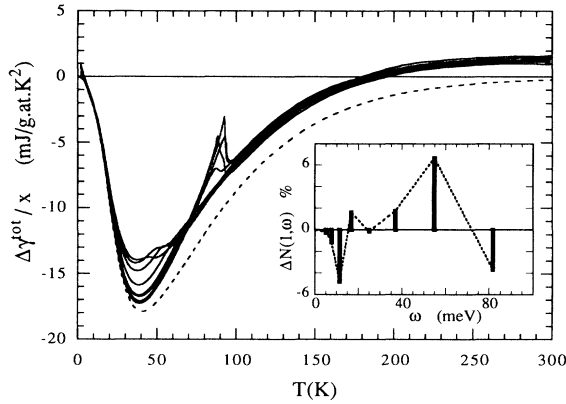


FIG. 2. $\Delta\gamma^{\text{tot}}/x$ vs T , where $\Delta\gamma^{\text{tot}} = \gamma^{\text{tot}}(x) - \gamma^{\text{tot}}(0)$, showing a normalized plot of data for $\text{YBa}_2\text{Cu}_3\text{O}_{6+x}$ relative to $\text{YBa}_2\text{Cu}_3\text{O}_{6.0}$ for ten conducting samples with $0.48 \leq x \leq 0.97$. The residual phonon term $\Delta\gamma^{\text{ph}}(1, T)$ for $x=1$ relative to $x=0$ (broken line) corresponds to the empirical discrete phonon spectrum $\Delta N(1, \omega)$ (inset). [Note that $\Delta\gamma^{\text{ph}}(T)$ reflects $\Delta N/\omega$.]

for several values of x , and $\gamma_{\text{ref}}^{\text{tot}}$ and $\gamma^{\text{tot}}(x, T)$ for $x=0$, 0.50, and 0.97 are shown in Fig. 1 (inset). For low values of the oxygen deficiency δ the phonon terms for the YBCO_{6+x} sample and fully oxygenated Zn doped reference are almost identical and $\gamma^{\text{tot}}(x, T) - \gamma_{\text{ref}}^{\text{tot}}(T)$ is dominated by their difference in electronic terms, as found previously [4]. With decreasing x a broad peak develops at around 40 K, increasing systematically with δ as the phonon spectrum softens. An approximately linear scaling of the residual phonon term with x may be deduced from Fig. 2 where we show a normalized plot of $\Delta\gamma^{\text{tot}}(x, T)/x$ for ten YBCO_{6+x} samples in the range $0.48 \leq x \leq 0.97$. Here $\Delta\gamma^{\text{tot}}(x, T) = \gamma^{\text{tot}}(x, T) - \gamma^{\text{tot}}(0, T)$ is the change in γ^{tot} relative to insulating $\text{YBCO}_{6.0}$ and is obtained by subtracting $\gamma^{\text{tot}}(x, T) - \gamma_{\text{ref}}^{\text{tot}}(T)$ for $x=0$ from the corresponding data for other x values. For $\text{YBCO}_{6.0}$ we expect electronic and 3D AF terms to be negligible as found for La_2CuO_4 [8] due to the charge-transfer gap and low magnetic dimensionality, and chain Cu(1) atoms are nonmagnetic for $x=0$. From the spin wave velocity [9] the 2D AF spin wave term $\gamma^{\text{SW}} \sim 1.8 \times 10^{-4}$ TmJ/g-at.K² is small below 300 K. Thus $\gamma(0, T) \sim 0$ and the electronic term $\Delta\gamma(x, T)$ of YBCO_{6+x} relative to YBCO_6 yields $\gamma(x, T)$.

It is evident from Figs. 1 and 2 that at high temperatures phonon terms converge and differences in γ^{ph} between two samples tend to zero. This results from the use of gram-atom units for γ . 1 g-at. contains Avogadro's number N_A atoms with $3N_A$ vibrational modes and $\gamma^{\text{ph}} \rightarrow 3R$ in the high temperature limit for any distribution of mode frequencies [1 g-at. $\equiv 1/(12+x)$ moles of YBCO_{6+x}]. At intermediate temperatures $\Delta\gamma^{\text{ph}}(x, T)$ reflects the difference $\Delta g(x, \omega)$ in phonon densities of states (PDOS) for sample and reference. The extreme breadth of the Einstein specific heat function ensures that

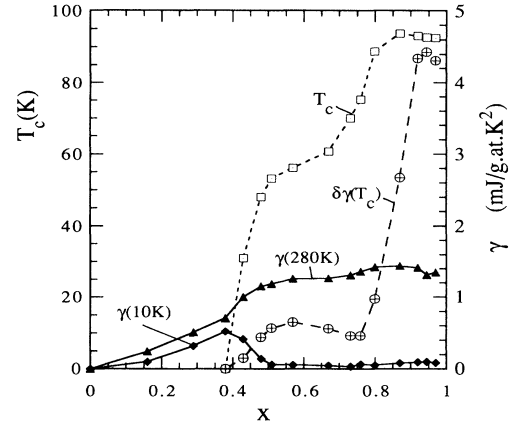


FIG. 3. Electronic specific heat parameters for $\text{YBa}_2\text{Cu}_3\text{O}_{6+x}$. Left-hand scale: T_c ; right-hand scale: $\gamma(x, 10 \text{ K})$, $\gamma(x, 280 \text{ K})$, and anomaly step height $\delta\gamma(T_c)$.

all structure in $\Delta g(x, \omega)$ is smoothed out and $\Delta\gamma^{\text{ph}}$ resembles dC^{ph}/dT . On general grounds $C^{\text{ph}} \propto T^3/\Theta_D^3$ and $\Delta\gamma^{\text{ph}} \propto T^2$ as $T \rightarrow 0$ and at high temperatures $C^{\text{ph}} = 3R(1 - \langle \omega^2 \rangle / 12T^2 + \dots)$ and $\Delta\gamma^{\text{ph}} \propto 1/T^3$. (The latter result ignores anharmonic and dilation terms but these largely cancel between two closely related samples.) Approximate values for the electronic term at low and high temperatures can be deduced by inspection of the raw differential data in Figs. 1 and 2 and more precise values obtained from plots of $\Delta\gamma^{\text{tot}}$ against T^2 or $1/T^3$. Values of $\gamma(10 \text{ K})$ and $\gamma(280 \text{ K})$ relative to $\text{YBa}_2\text{Cu}_3\text{O}_6$ determined from such plots are shown in Fig. 3.

There is no unique way of separating the phonon and electronic contributions at intermediate temperatures, but a simple procedure yields a residual phonon term consistent with changes in PDOS deduced from inelastic neutron scattering and electronic terms consistent with other properties. From the data for $x=0$ in Fig. 1, plots of $\gamma_{\text{ref}}^{\text{tot}}(T) - \gamma^{\text{tot}}(0, T)$ vs T^2 and $1/T^3$ yield approximately equal values for the electronic term $\gamma_{\text{ref}}(10 \text{ K})$ and $\gamma_{\text{ref}}(280 \text{ K})$ ($\sim 1.5 \pm 0.2$ and 1.4 ± 0.2 mJ/g-at.K², respectively). Assuming that $\gamma_{\text{ref}}(T)$ for this fully oxygenated 7% Zn sample is at most only weakly T dependent at intermediate temperatures [consistent with our [4] analysis of the total specific heat above T_c of Zn doped YBCO_7 ($0 \leq y \leq 0.1$) and that of Junod [1] for undoped YBCO_7] we obtain the residual phonon term $\Delta\gamma_{\text{ref}}^{\text{ph}}(T)$. Adding the small difference in phonon terms between 0% and 7% Zn doped $\text{YBCO}_{6.97}$ determined in Ref. [4] gives $\Delta\gamma^{\text{ph}}(0.97, T)$ for undoped $\text{YBCO}_{6.97}$ relative to $\text{YBCO}_{6.0}$. The corresponding normalized curve $\Delta\gamma^{\text{ph}}(1, T)$ in Fig. 2) is fitted empirically [10] by a discrete model spectrum $\Delta N(1, \omega)$ (Fig. 2, inset), then scaled with x and subtracted from each $\Delta\gamma^{\text{tot}}(x, T)$ to obtain each electronic term $\Delta\gamma = \gamma(x, T) - \gamma(0, T) \sim \gamma(x, T)$. Using a model difference spectrum with zero total number of modes and limited to the

known energy range of the phonon spectrum ensures that the T dependence of $\Delta\gamma^{\text{ph}}(1, T)$ is physically acceptable and allows a direct comparison with neutron scattering data. Inelastic neutron scattering measurements by Renker *et al.* [11] on YBCO_{6+x} reveal progressive changes in PDOS with x but little explicit temperature dependence of the spectrum. The discrete spectrum $\Delta N(1, \omega)$ shown in Fig. 2 (inset) is in excellent qualitative agreement with their observed change in generalized PDOS from $x=0$ to 1. Although linear scaling of $\Delta\gamma^{\text{ph}}(1, T)$ between $x=0$ and 1 provides a good approximation to the residual phonon term we find that linear scaling in the two ranges $0 < x < 0.3$ and $0.3 \leq x < 1$ with slightly different linear coefficients is required to completely remove $\Delta\gamma^{\text{ph}}$. Details of $\Delta\gamma^{\text{ph}}(x, T)$ and the almost identical phonon term changes with x in 2% and 7% Zn doped YBCO_{6+x} samples will be published separately. Correcting the data in Fig. 1 for $\Delta\gamma^{\text{ph}}(x, T)$ yields the electronic terms $\gamma(x, T)$ relative to that of YBCO_6 shown in Fig. 4. Any deviation of the true residual phonon term from the above quasilinear approximation will contribute to our derived curves for $\gamma(x, T)$ a broad term varying systematically with x and going to zero at low and high T . We see no clear evidence for such deviations.

The results for $\gamma(x, T)$ shown in Figs. 3 and 4 group broadly into the three regions identified in other properties, namely, the doped AF semiconductor $x < x_{\text{MI}} \sim 0.38$, and the "60 K plateau" ($0.48 < x < 0.76$) and "90 K plateau" ($0.80 < x < 0.97$) superconducting regions. $\gamma(x, 10 \text{ K})$ is small in the semiconducting region but exhibits a maximum at x_{MI} largely due to the peak in magnitude at x_{MI} of a low temperature upturn $\Delta\gamma^{\text{LT}}$. With the onset of superconductivity $\gamma(x, 10 \text{ K})$ falls sharply to $\sim 0.1 \pm 0.1 \text{ mJ/g-at.K}^2$ for $x \geq 0.48$. The variation of $\gamma(x, 10 \text{ K})$ with x is consistent with results for $\gamma(0)$ vs x of Nakazawa and Ishikawa [12] and is similar to the variation of $\gamma(0)$ with Sr content in $\text{La}_{2-y}\text{Sr}_y\text{CuO}_4$ [13].

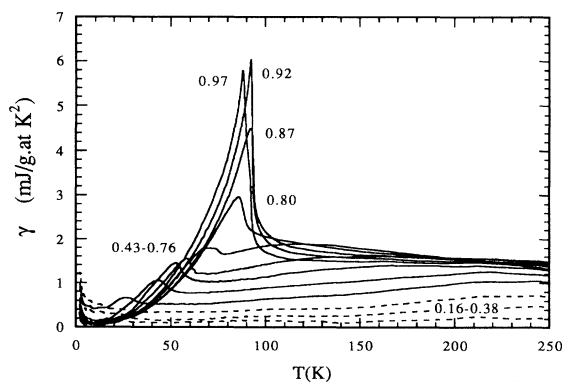


FIG. 4. Electronic specific heat coefficient $\gamma(x, T)$ vs T for $\text{YBa}_2\text{Cu}_3\text{O}_{6+x}$ relative to $\text{YBa}_2\text{Cu}_3\text{O}_6$. Values of x are 0.16, 0.29, 0.38, 0.43, 0.48, 0.57, 0.67, 0.76, 0.80, 0.87, 0.92, and 0.97.

Superconducting specific heat anomalies are observed over the entire superconducting region $0.43 \leq x \leq 0.97$. Transition temperatures T_c are in good agreement with resistive and magnetic determinations, and anomaly step heights $\delta\gamma(T_c)$ agree approximately with values quoted by Wühl *et al.* [14] and values estimated from reversible magnetization measurements by Däumling [15]. In the 60 K plateau region of T_c the anomalies are small but clearly defined with a maximum in $\delta\gamma(T_c)$ near $x=0.57$. Since $\gamma(x, 10 \text{ K})$ is close to zero the small step heights for $0.43 \leq x \leq 0.76$ cannot be attributed to a reduced superconducting volume fraction or to pair breaking (except for $x=0.43$), and it is therefore significant that the ratio $\delta\gamma(T_c)/\gamma_n \sim 0.5$ for this region of x is much less than the weak coupling BCS value 1.43. For the borderline compositions $x=0.73$ and 0.76 ($T_c=70$ and 75 K , respectively), the T dependence below T_c is consistent with an energy gap comparable to that of the 90 K plateau compositions, resulting in a large gap ratio $2\Delta(0)/kT_c \sim 7$ for these two samples. In the 90 K plateau region $x \geq 0.80$, T_c reaches a maximum value of 93.8 K at $x=0.87$ falling to 92.5 K for $x=0.97$, confirming that fully oxygenated YBCO_7 is slightly overdoped. Over the narrow range $0.76 \leq x \leq 0.92$ there is an order of magnitude increase in $\delta\gamma(T_c)$ with little change in T_c , as first observed by Junod *et al.* [16], and an increase in condensation energy $\propto \delta\gamma(T_c)T_c^2$ consistent with the factor 3 increase in thermodynamic critical field deduced by Däumling [15]. The anomalies for $x \geq 0.92$ have a magnitude $\delta\gamma(T_c)/\gamma_n \sim 2.5$ and temperature dependence below T_c typical of a strong coupling BCS superconductor with gap parameter $2\Delta(0)/kT_c \sim 5$, as found previously [4,17]. Gaussian fluctuations are clearly visible up to 120 K and their analysis [7] reveals a rapid increase in 3D character between $x=0.87$ and 0.97 .

There are significant changes in normal state T dependence of $\gamma(x, T)$ across the three regions. In the AF region $x < x_{\text{MI}}$ we find $\gamma(x, T) \sim \Delta\gamma^{\text{LT}} + B(x, T)$ with $B(x, T)$ increasing slowly with x and T . For $x_{\text{MI}} \leq x \leq 0.76$, $\gamma(x, T)$ shows substantial temperature dependence above T_c , exhibiting a broad peak moving to lower temperatures with increasing x . With further increase in x the normal state T dependence weakens rapidly, $\gamma(x, T)$ falling slightly above T_c to $\sim 1.4 \text{ mJ/g-at.K}^2$ at 280 K for $x \geq 0.92$. These results may be compared with the band structure value [18] $\gamma_{\text{bs}} = 1.0 \text{ mJ/g-at.K}^2$ for YBCO_7 . It is noteworthy that $\gamma(x, 280 \text{ K})$ increases smoothly through x_{MI} to a broad maximum or plateau at $x \sim 0.9$ (Fig. 3). No substantial increase is observed above 120 K for $x > 0.8$, excluding the possibility that the rapid variation of T_c or $\delta\gamma(T_c)$ in this region results from a 2D van Hove singularity close to the Fermi energy.

In spite of the complex changes in $\gamma(x, T)$ described above, a simpler continuity across the entire series is evident in plots of the entropy $S(x, T) = \int^T \gamma(x, T') dT'$ shown in Fig. 5 which suggests the evolution of a *single*

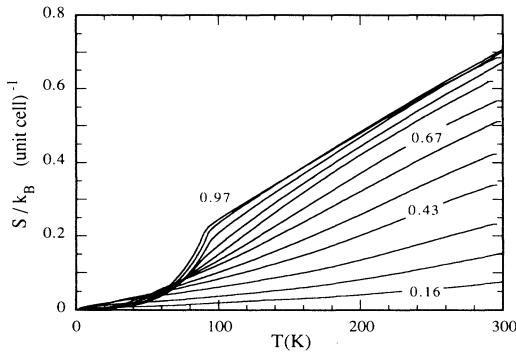


FIG. 5. Electronic entropy $S(x, T)$ for $\text{YBa}_2\text{Cu}_3\text{O}_{6+x}$. Values of x as in Fig. 4.

spectrum of excitations with x and T . Ignoring superconducting effects we observe a continuous progression from $S \propto T^n$ with $n > 1$ in the semiconducting region to $S \propto T$ as x approaches 1 with no abrupt change at x_{MI} , correlating with similar continuous changes in the ^{89}Y Knight shift [19] and bulk susceptibility [20]. This indicates that spin excitations may be important for all x and that the results are better described as a modification of the low energy spin spectrum with increased hole density and mobility than by a simple band model. Such behavior might result from the overdamping of 2D AF spin wave excitations by the holes. A rather rapid increase in low energy spectral weight in the heavily hole doped region would account for the increasingly linear T dependence of the entropy between T_c and ~ 200 K and the anomalous behavior of $\gamma(x, T)$ described above. The relevance of these results to the pseudogap behavior observed in various probes of the spin susceptibility will be discussed in a further publication.

From Fig. 5 we see that $S(T_c)$ in units of $k_B/(\text{unit cell})$ increases from ~ 0.06 for $x=0.57$ to 0.22 for $x=0.97$. These values are comparable with but somewhat lower than typical estimates of the hole density [increasing to $\sim 1/(\text{unit cell})$ for $x \sim 1$ or a factor 2 lower if the holes are paired at room temperature]. Bipolaron models propose preformed boson charge carriers Bose condensing at T_c and behaving classically at higher temperatures. Since the magnitude and T dependence of S indicates that the carriers are degenerate at 300 K, we find it hard to reconcile our results with this interpretation, but contrary views have been expressed [21–23]. Some versions of the t - J model of strongly correlated $\text{O}(2p)$ holes and $\text{Cu}(3d)$ spins predict decoupled holon (Bose) and spinon (fermion) excitations. If we attribute the bulk of the entropy at room temperature to the spinons we estimate from Fig. 5 an energy scale $T_0 \sim 1500$ K at which $S(T_0) \sim k_B$ per Cu, a value close to the exchange energy J as expected. However, unless this greatly overestimates the spinon entropy, little entropy is left for the Bose charge carriers. Indeed we see no evidence for independent excitations with different statistics. The

simplest interpretation of our results is that the carriers are fermions with a very low Fermi temperature ~ 1000 K, and that the condensate results from the k -space pairing of $\sim (10\text{--}30)\%$ of the Fermi sea.

In conclusion, the existence of an insulating end member YBCO_6 and the identification of changes in phonon specific heat consistent with neutron data and scaling with x have allowed a reliable determination of $\gamma(x, T)$ for the YBCO_{6+x} series. The results suggest a single spectrum of excitations for coupled holes and spins developing continuously between $x=0$ and 1 from spin-wave-like [$g(\omega) \sim \omega$] to Fermi-liquid-like [$g(\omega) = \text{const}$] with an energy scale $\sim J$. The magnitude and T dependence of the entropy suggest k -space pairing of fermion charge carriers for all x .

It is a pleasure to thank Sir Nevill Mott, J. M. Wheatley, and J. L. Tallon for helpful discussions and P. F. Freeman for sample preparation.

-
- [1] A. Junod, in *Physical Properties of High Temperature Superconductors*, edited by D. M. Ginsberg (World Scientific, Singapore, 1989), Vol. 2.
 - [2] N. E. Phillips, R. A. Fisher, and J. E. Gordon, *Prog. Low Temp. Phys.* **13**, 267 (1992).
 - [3] J. W. Loram, *J. Phys. E* **16**, 367 (1983).
 - [4] J. W. Loram, K. A. Mirza, and P. A. Freeman, *Physica (Amsterdam)* **171C**, 243 (1990).
 - [5] J. R. Cooper, S. D. Obertelli, A. Carrington, and J. W. Loram, *Phys. Rev. B* **44**, 12086 (1991).
 - [6] J. W. Loram, J. R. Cooper, and K. A. Mirza, *Supercond. Sci. Technol.* **4**, S391 (1991).
 - [7] J. W. Loram, J. R. Cooper, J. M. Wheatley, K. A. Mirza, and R. S. Liu, *Philos. Mag.* **B 65**, 1405 (1992).
 - [8] K. Sun *et al.*, *Phys. Rev. B* **43**, 239 (1991).
 - [9] J. Rossat-Mignod *et al.*, *Physica (Amsterdam)* **185–189C**, 86 (1991).
 - [10] J. W. Loram, *J. Phys. C* **19**, 6113 (1986).
 - [11] B. Renker *et al.*, *Z. Phys. B* **73**, 309 (1988).
 - [12] Y. Nakazawa and M. Ishikawa, *Physica (Amsterdam)* **162–164C**, 83 (1989).
 - [13] J. W. Loram, K. A. Mirza, W. Y. Liang, and J. Osborne, *Physica (Amsterdam)* **162–164C**, 498 (1989).
 - [14] H. Wuhl *et al.*, *Physica (Amsterdam)* **185–189C**, 755 (1991).
 - [15] M. Däumling, *Physica (Amsterdam)* **183C**, 293 (1991).
 - [16] A. Junod, D. Eckert, T. Graf, G. Triscone, and J. Muller, *Physica (Amsterdam)* **162–164C**, 482 (1989).
 - [17] J. W. Loram and K. A. Mirza, *Physica (Amsterdam)* **153–155C**, 1020 (1988).
 - [18] W. E. Pickett, *Rev. Mod. Phys.* **61**, 433 (1989).
 - [19] H. Alloul, T. Ohno, and D. Mendels, *Phys. Rev. Lett.* **63**, 1700 (1989).
 - [20] Y. Nakazawa and M. Ishikawa, *Physica (Amsterdam)* **158C**, 381 (1989).
 - [21] L. J. de Jongh, *Physica (Amsterdam)* **152C**, 171 (1988).
 - [22] N. F. Mott, *Philos. Mag. Lett.* **63**, 319 (1991).
 - [23] A. S. Alexandrov and J. Ranninger, *Solid State Commun.* **81**, 403 (1992).